OXIDATION MECHANISMS OF CASTABLE REFRACTORIES FOR BLAST FURNACE RUNNERS.

1- Silvia Camelli*
2- Elena Brandaleze**
3- Jorge Madias***
4- Raul Topolevsky****

ABSTRACT

A study on castables refractories used in Blast Furnaces runners is presented. The objective is to increase the knowledge on the behavior of this type of materials. This study includes a characterization of the refractory material, both before and after use. The analysis of the sintering reaction, the study on silicon carbide dissociation and the thermodynamical interpretation on the SiC-C-O system, jointly with the post mortem study results permitted to identify the carbon oxidation mechanisms of the several runner zones. Finally, the equilibrium phase diagram analysis and thermal profile diagram of the blast furnace runner let us to establish key factors on castable refractory wear in service.

KEYWORDS blast furnace, runner, wear, thermal profile.

1. INTRODUCTION

The objective of this work is the determination of the wear mechanism by oxidation of blast furnace (BF) runners and the increase of the knowledge on the behavior of these materials. A characterization is carried out on samples of castable refractory without use (WU) and after use (PM).

The analysis of sintering reactions, SiC dissociation and SiC-C-O system is made. This way, the carbon oxidation mechanisms that prevail in different areas of the runner are identified. The cement bonding of the ultra low cement castable material (ULC) is studied during dewatering, drying and sintering. These issues are relevant to the lining practice.

Lastly, the crystalline phases in these materials are identified. The wear rate and sintering rate of these castables are determined.

1º Encontro Internacional sobre Redução - ABM

* Siderar SAIC
** Instituto Argentino de Siderurgia – Refractarios
*** Instituto Argentino de Siderurgia – Acería
**** Siderar SAIC

CASTABLES CHARACTERIZATION

The castables characterization is carried out on "without use" and "post mortem" samples that were extracted of different areas in the BF runner. The different stages involved in this study are:

- Crystalline phases identification by DRX
- Density and apparent porosity determination
- Chemical analyses by means of EDS, the energy dispersive spectrometer technique.
- Observation of samples on light microscope and scanning electronic microscope. (SEM).
- Analysis of the behavior of the coal blend.

The evaluation of the oxidation resistance of the coal blend is carried out by means of C analysis and the calcining loss by means of DTA and TGA.

SINTERING REACTIONS

The analysis includes:

- Evaluation of binder (calcium aluminate, calcium silicoaluminate and others), carried out through the study of the Al_2O_3-CaO-SiO_2 system
- A study on the interaction between slag or hot metal with the refractories
- Analysis of temperature influence on the reactions

SiC DISSOCIATION ANALYSIS

A study of the SiC – O, and CSi/SiO_2/O_2 in front of C/CO_2/CO/O_2 system is carried out.

2. DEVELOPMENT

Chemical analysis and physical properties of two castables used as working lining in BF runners are presented in table I.

Characteristics	**Castable Refractory**	
Chemical composition	**A**	**B**
Al_2O_3 (%)	67.1	68 / 75
SiO_2 (%)	4.2	6 max
SiC (%)	24.0	18.5 / 23
C (%)	2.0	-
CaO (%)	-	1 max
Fe_2O_3 (%)	-	0.50 max
Specific weight (g/cm^3)	3	2.82 / 3.03
Apparent porosity (%)	-	8.5 / 13.5
Cold Compression Strength		
After drying (110°C 2h)	50 MPa	25 / 60 MPa
After heating (A: 1500°C; B: 1400 °C)	70 MPa	40 / 80MPa
Permanent Linear Variation		
After drying (110°C 2h)	-	-0.2 / 0.3 %
After heating (A: 1500°C; B: 1400 °C)	0.2 %	-0.2/0.4 %

Table I. Main blast furnace runners castable refractories characteristics.

In table II crystalline phases identified by DRX, as well as density and apparent porosity of castable A and B are presented.

Castable	**Crystalline Phases**	**Density** (g/cm^3)	**Apparent Porosity** (%)
		Kerosene	**Kerosene**
A	α-Al_2O_3 SiC (12H) SiC (8H) SiC (4H) α-SiC Si α-SiO_2	2.95	7.91
B	α-Al_2O_3 SiC (12H) SiC (8H) Si α-SiO_2	2.89	12.2

Table II. Crystalline phases, density and porosity of castable refractories A and B.

In the table III EDS analysis for constituents of castable A are presented, as well as C analysis and calcining loss.

Sample	**Al_2O_3** (%)	**SiO_2** (%)	**CaO** (%)	**TiO_2** (%)	**FeO** (%)	**Calc. loss** (%)	**C** (%)
M 1	42.7	56.1	-	1.25	-	2.95	6.80
M 2	75.9	-	24.1	-	-	-	-
M 3	38.	62	-	-	-	-	-
M 4	49.7	46.0	1.4	1.6	1.3	-	-

Table III. EDS analysis, C% and calcining loss on samples M1, M2, M3, M4 of castable A.

M1 as conformed
M2 aluminate cement
M3 refractory grains
M4 as received

2.1. POST MORTEM STUDY

The PM samples were extracted from the runner on three areas (figure 1).

- **Cold face of refractory in contact with air** (high oxygen potential area):
- **Cold face of refractory in contact with slag:** sample II
- **Cold face of refractory in contact with hot metal** (low oxygen potential): sample III.

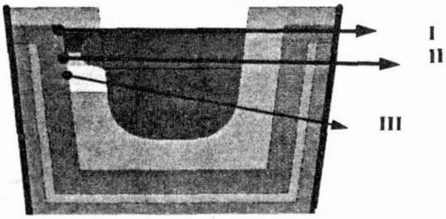

Figure 1. Location of samples I to III taken for post mortem study.

Sample I was taken 6 m away from the taphole (figure 2, left). Sample II, corresponding to slag line, is shown in figure 2, right.

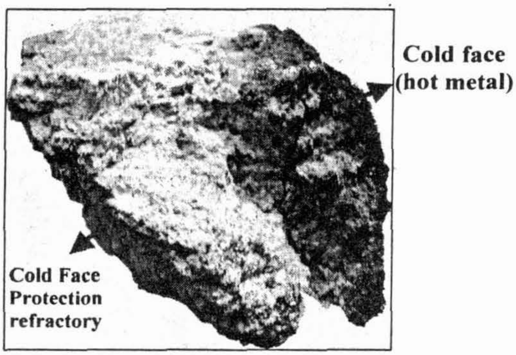

Figure 2. Sample I, extract from 6 m of the tap hole, in the high oxygen potential zone.

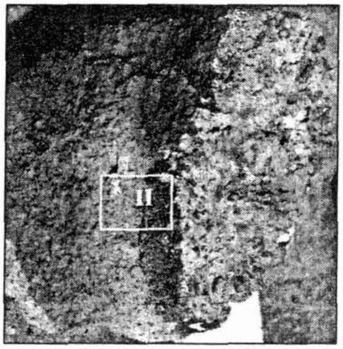

Figure 3. Sample II, extracted of the slag line.

Sample III, taken from the refractory in contact with the hot metal, is shown in figure 4.

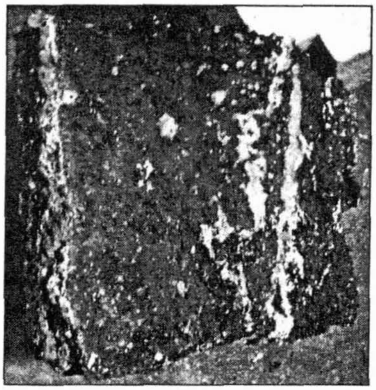

Figure 4. Sample III, taken from the refractory in contact with hot metal.

In table IV crystalline phases, density, porosity, calcining loss and C% are detailed for each of the three samples.

Sample	Crystalline Phases	Density (g/cm^3)		Porosity (%)		Calcin. Loss (%)	C (%)
		H_2O	K	H_2O	K		
I	α-Al_2O_3; SiC (12H); SiC (8H) SiC (4H) α-SiC Si α-SiO_2	2.68	2.68	24.4	24.4	0	6.63
II	α-Al_2O_3 SiC (12H) SiC (8H) SiC (4H) α-SiC; Si	2.79	2.75	19.5	21.53	1.21	6.73
III	α-Al_2O_3 SiC (12H) SiC (8H) SiC (4H) α-SiC C (graphite) $3Al_2O_32SiO_2$	2.94	2.88	11.7	14.8	4.18	5.97

Table IV. Crystal phases, porosity, density, calcining loss and C content on the three samples for post mortem study.

2.2. THERMODYNAMIC ANALYSIS OF SiC STABILITY

First, SiC stability is analyzed by taking into account SiC-O system; then by the SiC-C system and finally the effect of the CO/CO_2 ratio in the atmosphere is discussed.

2.2.1. SiC - O system.

From the thermodynamic point of view, silicon carbide is not stable in presence of air at room temperature. It reacts with the oxygen, forming other components of smaller free energy. However, in practice the silicon carbide is stable due to the very slow rate of reaction kinetics. But at high temperature SiC oxidation can be very significant [1].

According to the oxygen content in the atmosphere in contact with SiC, different reaction products are obtained. For example, in presence of an oxygen rich atmosphere, the reaction products will be SiO_2 and CO_2 or SiO_2 and C, [2]. But if oxygen content is limited, the products can be $CO_{(g)}$, $SiO_{(g)}$ or Si. In table V the possible reactions between silicon carbide and oxygen are presented [1].

$SiC + 2O_2 \longrightarrow SiO_2 + CO_2$
$SiC + {}^{3}/_{2}$ O2 $\longrightarrow SiO_2 + CO$
$SiC + O_2 \longrightarrow SiO_2 + C$
$SiC + {}^{3}/_{2} O_2 \longrightarrow SiO + CO_2$
$SiC + O_2 \longrightarrow SiO + CO$
$SiC + \frac{1}{2} O_2 \longrightarrow SiO + C$
$SiC + O_2 \longrightarrow Si + CO_2$
$SiC + \frac{1}{2} O_2 \longrightarrow Si + CO$

Table V. Possible reactions between SiC and O_2.

In table VI each one of the possible reactions by oxygen mole and the corresponding equations of free energy with temperature variation are presented.

Reactions per mole of O_2	**$\Delta G°$ [Kcal]**	**No.**
$\frac{1}{2} SiC + O_2 \rightarrow \frac{1}{2} SiO_2 + \frac{1}{2} CO_2$	-147,19 + 0,0203T	①
${}^{2}/_{3} SiC + O_2 \rightarrow {}^{2}/_{3} SiO_2 + {}^{2}/_{3} CO$	-152,1 + 0,0135T	②
$SiC + O_2 \rightarrow SiO_2 + C$	-199,97 + 0,0404T	③
${}^{2}/_{3} SiC + O_2 \rightarrow {}^{2}/_{3} SiO + {}^{2}/_{3} CO_2$	-68,63 + 0,0123T	④
$SiC + O_2 \rightarrow SiO + CO$	-36,73 + 0,0387T	⑤
$2\ SiC + 1/2O_2 \rightarrow 2\ SiO + 2\ C$	-17,06 + 0,0372T	⑥
$SiC + O_2 \rightarrow Si + CO_2$	-78,56 + 0,0012T	⑦
$2\ SiC + O_2 \rightarrow 2\ Si + 2\ CO$	-24,72 + 0,044T	⑧

Table VI. Free Energy variation for the reactions of SiC in presence of O.

To find the range of stability for these reactions, the variation of free energy in function of temperature is represented (figure 6). A nomographic scale that permits to calculate the partial pressure of the oxygen is also included. In accordance with the diagram, the more stable reaction up to 1506°C is number (3). At higher temperatures the stable reaction is number (2).

At low temperatures, i.e. T = 927°C, the oxygen partial pressure ($P^e\ O_2$) required for silicon carbide oxidation is 3.8×10^{-28} atm, that is to say, at pressures of oxygen higher than equilibrium, the oxidation of SiC is favored (by generating of SiO_2 and C). On the other side, for smaller oxygen pressure SiC is more stable.

Up to 1377 ° C the oxygen partial pressure (P^eO_2) necessary for silicon carbide oxidation is 2.8×10^{-18} atm. Therefore, the higher the temperature, the higher the oxygen partial pressure required for silicon carbide dissociation.

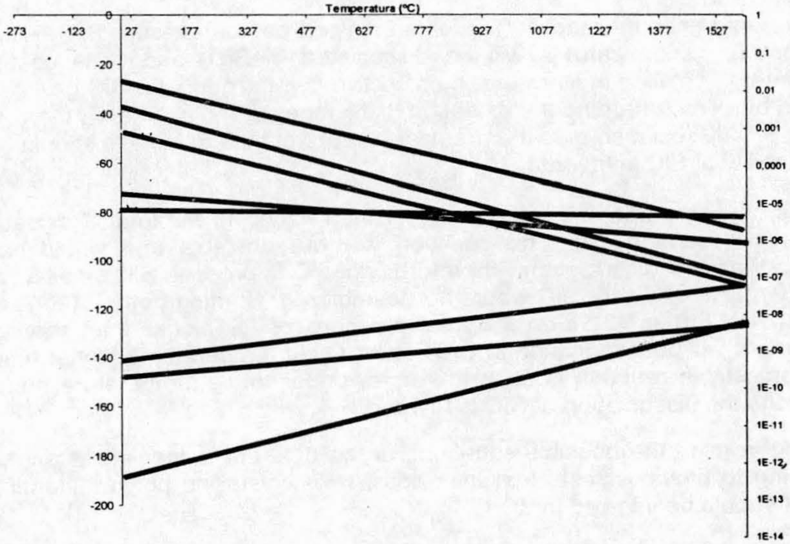

Figure 6. SiC stability in front of oxygen according to Ellingham diagram.

2.2.2. SiC-C-O system.

The refractory castable besides silicon carbide contains 2 to 5% carbon. In table VII the possible reactions of carbon with oxygen are presented. In figure 7 the Δ G ° - T diagram corresponding to these reactions is detailed.

$C_{(s)} + O_{2\,(g)} \rightarrow CO_{2\,(g)}$	⑨
$C_{(s)} + O_{2\,(g)} \rightarrow 2CO_{(g)}$	⑩

Table VII. C reactions with O_2

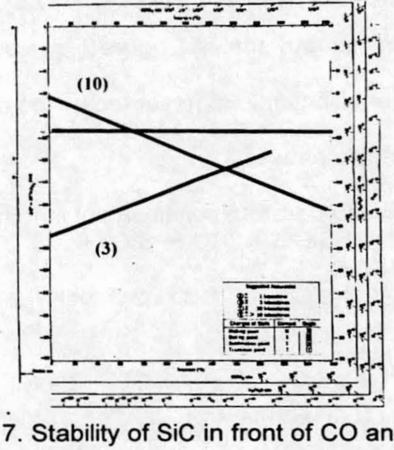

Figure 7. Stability of SiC in front of CO and CO_2.

At constant temperature, i.e. at 927°C:

➢taking into account reaction (3) for an oxygen partial pressure $P^eO_{2\,(I)}$ higher than equilibrium, silicon carbide will be dissociated in SiO_2 and C. According to the experiments detailed in literature, a protective layer around the SiC grains should be formed by silica, retarding the oxidation. If it is considered as total C, the C generated during SiC dissociation plus the graphite content of the castable, it should be inferred that stability of SiC is favored.

➢If the oxygen partial pressure is bigger than P^eO_2 (II), the total C oxidation to CO will begin (equation 10). This reaction is more unstable and would have faster kinetics than SiC dissociation. Therefore, while C is present, SiC stability is favored. But when C is oxidized, SiC would be destabilized. Starting from 1506°C, the stable reaction for SiC is (2). For a partial pressure of O_2 bigger than the equilibrium pressure, it will be dissociated in SiO_2 and CO. At temperatures higher than 1515°C the more stable reaction is (10); therefore, under these temperature and pressure conditions the dissociation of SiC is favored.

Keeping in mind the possible situations at the different runner areas analyzed, and according to previous tests (calcining loss, C%, crystalline phases identification by DRX) it should be inferred that:

- **Sample I** (high O_2 potential area):

At low temperature and high oxygen content, a progressive oxidation of C occurs and SiC remains stable. This stability could be associated to a very slow kinetics of the oxidation reaction, or insufficient time and temperature.

- **Sample II:** (slag line area)

At 1200°C and low oxygen content, an oxidation of 60% of the C would occur and SiC remains stable.

- **Sample III:** (hot metal area)

In this area there is high temperature and low O_2 potential. Hence, recarburization of the refractory in contact with hot metal takes place and silicon carbide dissociation begins.

2.2.3. SiC / SiO_2 / O_2 EQUILIBRIUM IN FRONT OF C / CO_2 / CO / O_2 SYSTEM.

According to Ellinghamm diagram analysis, figure 7, it is possible to say that:

- **At T <700 ° C.**

CO_2 is more stable CO; equilibrium is represented by the reaction:

$$SiC + CO_2 \rightarrow SiO_2 + 2\,C$$

Being SiO_2 is the most stable phase.

- **At 700 ° C <T <1506 ° C.**

SiO_2 is more stable in this temperature condition but in front of the CO the reaction is:

$$SiCO + 2CO \rightarrow SiO_2 + 3\,C$$

- **At 1506 ° C <T <1515 ° C**

$$2/3\ SiC + 4/3\ CO \rightarrow 2/3\ SiO_2 + 2C$$

- **At T> 1515 ° C**

CO is the more stable phase.

$$2/3\ SiO_2 + C \rightarrow 4/3\ CO + 2/3\ SiC$$

At temperatures lower than 1515°C, SiC reacts with CO_2 and CO to form SiO_2 and C. The protective layer of silica is formed and it avoids the deep oxidation of the SiC.

But at temperatures higher than 1515°C, this layer is broken and the SiC leaves exposed.

2.2.4. THE ATMOSPHERE TYPE EFFECTS. (CO/CO_2 ratio)

For any temperature value within the normal operating range, a $CO/CO_2 = 1$ ratio will not favor the silica reduction, that is to say it results an oxidizing atmosphere for SiC. It is necessary to modify the CO/CO_2 ratio to achieve a reducing atmosphere. For instance, equilibrium between SiC and SiO_2 at 900 ° C in a CO/CO_2 atmosphere can be represented by the equation

$$SiC + 2\ CO_2 \rightarrow 2\ CO + C + SiO_2$$

At 900 ° C, CO/CO2 ratio is 10^6. Therefore, SiO_2 oxide will be reduced and SiC will remain stable if the CO/CO_2 ratio is bigger than 10^6. But if CO/CO_2 ratio is lower than 10^6 the stable phase will be SiO_2.

2.3. PHASE DIAGRAMS ANALYSIS.

The castable refractory matrix is constituted for aluminate and microsilica cement. These microparticles occupy the free spaces between the cement grains and the other cement polycrystalline particles. They improve the efficiency on the packaging of the particles since the water is replaced by these additives and high density, low porosity and good mechanical strength of the castable are obtained as a result [3]. Microsilica is used to reduce the water content of the low cement concrete. By replacing water and air between fines fluidity of concrete is improved [4]. Also, microsilica promotes mullitization of the matrix in service. So, resistance to slag corrosion and mechanical strength at high temperature are increased [5]. In figure 8, the Al_2O_3-CaO-SiO_2 system is presented, including the location of matrix of castable A and B, and slag, by EDS analysis.

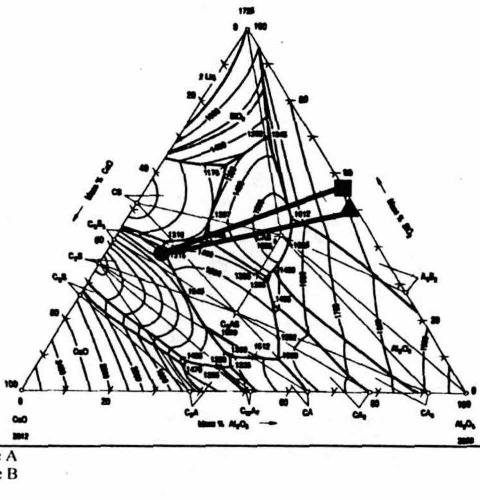

▲ matrix of castable A
■ matrix of castable B
● Slag

Figure 8. Slag and matrix of castable A and B located in the Al_2O_3 - CaO - SiO_2 system.

The amount of liquid formed in the castable at each temperature can be calculated (figure 9). Analyzing the compatibility between the slag and matrix of the castable, a considerable increment of the percentage of liquid is observed at the equilibrium on slag - matrix interface. The methodology applied for this analysis was developed by Dr. De Aza [6]. He considered a relation of 5% slag and 95% of matrix on the refractory material.

Then, at equilibrium when castable is in contact with slag, liquid in the matrix is increased, as compared with the matrix evolution without slag presence (figure 9).

In order to understand in detail the influence of a certain liquid phase percentage on the sintered thickness in the castable after use, an analysis is made keeping in mind the following point:

T_{PC} is the temperature at which the castable reaches its highest mechanical strength at high temperature.

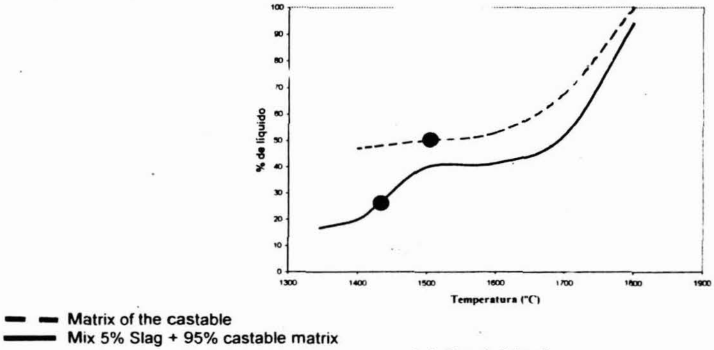

(a) Castable A.

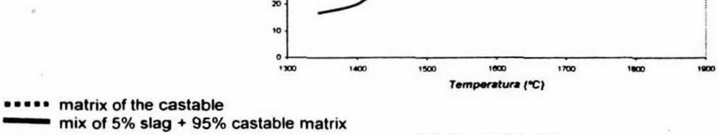

(b) Castable B.

Figure 9. Liquid percentage present in castable matrix at different temperatures. *Top: Castable A. Bottom: Castable B.*

When the matrix enter into contact with the slag, the liquid portion in equilibrium with the matrix of the castable is considerably increased in comparison with the matrix evolution without slag presence. If temperature profile on the BF lining runner is analyzed, where T = Tpc temperature it is possible to evaluate the sacrifice thickness of the refractory castable. It is relevant to mention that sacrifice thickness is defined as the minimum thickness of the refractory castable that will be sintered or mullitized to achieve enough resistance to wear and corrosion to keep balance between erosion and sintering rate.

This methodology allows to obtain qualitative information of the behavior of the castable refractory in service and to bring about a comparison between two or more refractory materials.

In figure10 Tpc temperature for each castable under study is represented, on the background of the working lining temperature profile. These figures allows us to extract the following conclusions:

∴ At higher Tpc the sintered thickness is smaller for castable A than for castable B.
∴ When thermal profile changes, for instance due to an increase of temperature in the cold face of the lining, the sintered thickness decreases.
∴ An increment of Tpc, for a given castable, implies that:
  * Sacrifice thickness decreases
  * Smaller sintered layer
  * Higher erosion rate

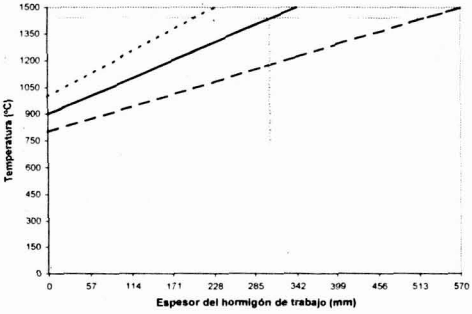

(a) Sacrifice Thickness for Castable A

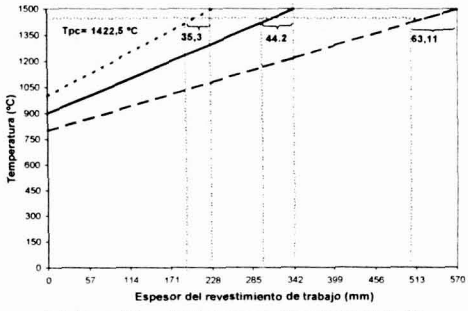

(a) Sacrifice Thickness for Castable B

Figures 10. Estimation of sacrifice thickness in function of Tpc for a given thermal profile.
Top: Castable A. Bottom: Castable B.

3. CONCLUSIONS

The SiC-C-O system thermodynamic study, jointly with the results obtained in the post mortem study of refractory castables, allowed to identify the carbon oxidation mechanisms that prevail in the different areas of the runner.

In the castables that were studied, the SiC remained stable up to 1200°C. SiC stability could be associated to a very slow kinetics of the oxidation reaction, or insufficient time or temperature. On the other side, under high temperature conditions SiC dissociation is observed, in spite of a lower O_2 potential.

The phase diagrams and the thermal profile analysis of the BF runner let us establish

* the evolution of composition on the matrix
* the distance to the hot face
* the cold face temperature
* the interaction between the concrete and the slag
* the sintered thickness of the castable.

BIBLIOGRAPHY.

1 G. Ervin. Oxidation Behavior of Silicon Carbide. Journal of The American Ceramic Society. Vol. 41, N° 9, pp. 347-352.

2 K. Kreuels, I. SteinneBen. Development of Blast Furnace Trough Castables. Aachen Proceedings 1988, pp. 95-97.

3 T. Bier, N. Bunt, C. Parr. Calcium Aluminate Bonded Castables: Their Advantages and Applications. XXV Congreso ALAFAR, 1996.

4 M. Ishikawa. Refractory Castables. Taikabutsu Overseas, Vol. 19 N° 3, Sep. 1999.

5 M. Caligaris, L. Zamboni, N. Quaranta y R. Caligaris. Estudio Post Morten de hormigones de alta alúmina. Cerámica y Cristal 119. Febrero de 1997. 23-25.

6 Vicente, P. Pena, S. De Aza. Aplicación de los diagramas de equilibrio de fases a la evaluación del comportamiento de los materiales de SiO_2-Al_2O_3 frente a escorias con relaciones CaO/SiO_2 variables. Bol. Soc. Esp. Ceram. Vidr. 25 (1986) 2, 97-103.